



Universidad Autónoma  
de Madrid

**Biblos-e Archivo**  
Repositorio Institucional UAM

**Repositorio Institucional de la Universidad Autónoma de Madrid**  
<https://repositorio.uam.es>

Esta es la **versión de autor** del artículo publicado en:  
This is an **author produced version** of a paper published in:

Environmental Geochemistry and Health 42.7 (2020): 2147-2161

**DOI:** <https://doi.org/10.1007/s10653-019-00485-2>

**Copyright:** © 2019 Springer Nature B.V.

El acceso a la versión del editor puede requerir la suscripción del recurso  
Access to the published version may require subscription

# Impact of a tire fire accident on soil pollution and the use of clay minerals as natural geo-indicators

Jaime Cuevas<sup>1</sup>, Daniel E. González-Santamaría<sup>1\*</sup>, Carlos García-Delgado<sup>1</sup>, Aitor Ruiz<sup>1</sup>, Antonio Garralón<sup>2</sup>, Ana I. Ruiz<sup>1</sup>, Raúl Fernández<sup>1</sup>, Enrique Eymar<sup>3</sup>, Raimundo Jiménez-Ballesta<sup>1</sup>

<sup>1</sup> Department of Geology and Geochemistry. Autonomous University of Madrid, 28049 Madrid; [jaime.cuevas@uam.es](mailto:jaime.cuevas@uam.es), [daniel.g.santamaria@uam.es](mailto:daniel.g.santamaria@uam.es); [carlos.garciadelgado@uam.es](mailto:carlos.garciadelgado@uam.es); [aitor.ruiz@estudiante.uam.es](mailto:aitor.ruiz@estudiante.uam.es); [anai.ruiz@uam.es](mailto:anai.ruiz@uam.es); [raul.fernandez@uam.es](mailto:raul.fernandez@uam.es); [raimundo.jimenez@uam.es](mailto:raimundo.jimenez@uam.es)

<sup>2</sup> Department of environmental, CIEMAT, Avda. Complutense, 22, 28040 Madrid (Spain); [antonio.garralon@ciemat.es](mailto:antonio.garralon@ciemat.es)

<sup>3</sup> Department of Agricultural Chemistry and Food Sciences. Autonomous University of Madrid; [enrique.eymar@uam.es](mailto:enrique.eymar@uam.es)

\* Correspondence: [daniel.g.santamaria@uam.es](mailto:daniel.g.santamaria@uam.es); Tel.: 34-91-4975769; 28049 Madrid (Spain) ORCID: 0000-0002-1175-9763

**Abstract:** Following the occurrence of a fire at a tire landfill in the surrounding area of Madrid City (Spain), polycyclic aromatic hydrocarbons (PAHs) and trace elements present in soils were analysed to assess the impact of the fire. The capacity of the soils' clay mineral fraction to reflect this air pollution incident was studied. Fourteen soil samples were collected at different distances under the smoke plume, and they were subjected to High-Performance Liquid Chromatography–Photodiode Array Detection (HPLC–PAD), Inductively Coupled Plasma Mass Spectrometry (ICP–MS) and X-Ray Diffraction (XRD) analyses. Clay minerals content showed a strong correlation with the pollutants potentially released in the tire fire, acenaphthene, pyrene, benzo(a)pyrene, and benzo(a)fluoranthene. Trace metals Zn and Se were related to the proximity of the tire fire without any relationship to clay minerals content. This work suggests the use of natural clay minerals as potential PAHs geo-indicators in response of air pollution, complementary to current air and biological analyses.

**Keywords:** Clay minerals; tire fire landfill; health and environmental risk; pollution-monitoring; PAHs; hazardous trace elements.

## 1. Introduction

Lasting 23 days, a fire occurred in an illegal tire landfill, which was located in the vicinity of Seseña (Toledo, Spain), near the border between the two Spanish Autonomous Communities of Madrid and Castilla-La Mancha. The tire landfill had an extension of 117,000 m<sup>2</sup>, and around 70,000–90,000 tons of tires were stored there. Tires are widely used products and a great quantity of them are scrapped and deposited on different types of soils, causing massive accumulations, which generates an ever-growing problem in many regions worldwide. In recent decades, several tire fires have occurred, e.g., (Downard et al. 2015; Steer et al. 1995; Wang et al. 2007), representing a potential health and environmental risk as a result of the production of toxic chemical products. The gas and particulate matter emissions reach the atmosphere and can be transported by the wind across large distances (from meters to hundreds of kilometres) until their wet (rain precipitation) or dry deposition onto the soil.

Tires are made with more than 100 different substances (Seidelt et al. 2006): mainly rubber (50 wt. %), carbon black or silica gel (25 wt. %), steel (10 wt. %), sulphur (1 wt. %), ZnO (1 wt. %) and many other additives. This complex mixture promotes the occurrence of combustion and pyrolysis processes, which release a wide variety of hazardous pollutants such as polycyclic aromatic hydrocarbons (PAHs) and hazardous trace elements. PAHs are a group of organic molecules

composed of 2-7 fused aromatic rings and they have particularly relevance due to their bioactive, toxic and persistent effect (Akhbarizadeh et al. 2019). Trace elements can be classified as “essential” being required in low concentrations for human health (e.g., Cu, Zn Fe, Co, and Se), “probably essential” which their role in human metabolism is unproven (e.g., Ni, V, and B) or “not essential” and toxic for human metabolism (e.g., As, Hg, Cd, and Pb). However, the exposure to a high levels of any metal lead to toxic effects, particularly “not essential”, which are toxic, even a very low concentration.

Several authors have studied the tire fire accident in Seseña (Artiñano et al. 2017; Escobar-Arnanz et al. 2018; Nadal et al. 2016), which is the object of this paper. In these works, sampling campaigns were carried out during the tire fire, and once it was extinguished the researchers reported high concentrations of ZnO,  $\text{SO}_4^{2-}$ , PAHs, volatile organic compounds (VOCs), and increases in the background levels of trace elements, such as As, Cr, Cu, Co or Zn. These studies carried out a characterization of the soil, air samples (including particulate matter and deposited dust), and plants collected in the surroundings. The present study focusses on the footprint left on the soil surface, with special attention to the clay minerals particles present in the soil and their potential capacity to store information about the air-pollution episode. Clay minerals are naturally widely distributed, they have numerous applications in a large number of areas such as health, engineering, or industrial among others, but in the last years, their interest for pollution control and environmental protection have grown (Bergaya and Lagaly 2013).

In the present work, several soil samples, which contained clay minerals were analysed to determine PAHs and hazardous trace elements as the main pollutants, whereas X-Ray Diffraction (XRD) was used to perform semi-quantitative determinations of clay minerals.

While the impact of fires on vegetation and wildlife is obvious, by contrast, the impact of fires on soils is less obvious and multi-disciplinary approaches improve the management of complex and uncertain situations (Stewart and Hursthouse 2018). Soil is a complex, heterogeneous medium comprising mineral and organic solids. In the sampling area, organic contents are scarce, so its role as an absorbent is lower than in the rich organic matter soils. In contrast, natural clay minerals are considered some of the most reactive components of soils (Hundal et al. 2001), useful for de-pollution and pollution controller (Churchman et al. 2006). Clay minerals are layered, nanostructured materials, with a fine size particle ( $< 2 \mu\text{m}$ ), which brings relevant properties such as surface charge, surface area, and reactive surface groups. For example, illite (Ilt) (Swift and McLaren 1991), and particularly the smectite group (Sm) of clay minerals, have a strong affinity for heavy metal ions as  $\text{Cu}^{2+}$ ,  $\text{Zn}^{2+}$ ,  $\text{Cd}^{2+}$ , or  $\text{Ni}^{2+}$ . This ion uptake involves a variety of processes: simple ion exchange, surface complexation and surface precipitation. Moreover, clay minerals can also absorb a significant amount of gases (Volzone 2007); their high-surface areas and volume of fine pores enable them to adsorb non-ionic volatile substances. The existence of non-charged interlaminal surface sites induce them to form hydrophobic bonds with organic pollutants. Much recent research has studied the capability of natural clay minerals to trap PAHs such as phenanthrene (Phe) and pyrene (Pyr), (e.g., González-Santamaría et al. 2017; Cobas et al. 2014).

The target of this work is to obtain a preliminary screening of the impact caused by the tire fire, especially attending to toxic levels. On the other hand, we hypothesize the potential of clay minerals as geo-indicators of soil contamination during a tire fire episode.

The present paper intend to show the potential use of clay minerals, in significant content of some of the analysed soils to detect the emission of pollutants from the tire fire. Due to the harmful substances released from tyre fires and the ability of clay minerals to trap pollutant gases (Volzone 2007), this study focussed in these minerals present in soils, which can provide a valuable information for risk monitoring.

79

80 **2. Materials and Methods**

## 81 2.1. Sampling conditions

82 The sampling campaign was conducted on 15 May 2016, the third day after the beginning of the accident. Weather  
 83 conditions were unstable; before the start of the tire fire, brief drizzles occurred (MeteoValdemoro 2016). The prevailing  
 84 wind compound changed on the third day from west to east, and the average wind speeds were 8.0, 4.8 and 3.2 km/h for  
 85 the first three days, respectively.

86 Geologically, the area is located in the Neogene Madrid Basin, in lacustrine and palustrine sediments from Miocene.  
 87 This area is characterized by clay, carbonate and gypsum beds intercalated with many areas of geogenic sedimentary  
 88 environments (Bustillo and Alonso-Zarza 2007). These sediments are of special interest because they contain deposits of  
 89 Mg-clays, consisting of sepiolite and non-fibrous Mg-clay minerals like saponite, stevensite and kerolite–stevensite mixed  
 90 layers (Clauer et al. 2012), which are classified within the Sm group of clay minerals. From a pedological point of view,  
 91 the soils under and around the tire landfill are Xerorthents (USDA 2014) or Regosols (FAO 2015), under scarce vegetation  
 92 protection.

93 The sampling procedures were based on judgmental sampling (Swyngedouw and Crépin 2008), which applies  
 94 presumptions about the behaviour (movement and distribution) of pollutants according to the slope, time distance, and  
 95 knowledge of the area. Thus, 14 soil samples were collected at different distances from the tire fire under the influence  
 96 area of the smoke plume. The crust of the soil surface with a depth of (~1–5 cm) was collected using a stainless steel pallet.  
 97 The location area and the distribution of sampling points (Sp1–14) is shown in Fig. 1. Sp1 and Sp2 were located at ~15,000  
 98 m from the tire fire, in farmlands and in front of a road (~400 m). Sp3 and Sp6 were located at 9,300 m and 7,100 m,  
 99 respectively, at the slope facing the road. Sp4 and Sp5 were placed at 8,800 m from the tire fire, in cropland. Sp7 and Sp8  
 100 also were positioned at ~2,500 m, also in farmland. Sp10 and Sp9 were placed in croplands at 500 m from the tire fire.  
 101 Sp11 was located at ~200 m from the edge of the landfill. Finally, Sp13, Sp12 and Sp14 were placed in a scarp next to the  
 102 tire fire. The geographic altitudes registered for the sampling points ranged from 707 and 712 m (Sp11, Sp12, Sp13, Sp14),  
 103 677 m (Sp9, Sp10), 636 m (Sp6), 645 m (Sp4, Sp5), 634 (Sp3), 612 m (Sp7, Sp8) and 571 m (Sp1, Sp2). Once collected,  
 104 all samples were put into glass jars and stored in the absence of light at < 5 °C.

105

## 106 2.2. Mineralogical analyses

107 In order to study the mineralogical composition, a sufficient quantity of sample was dried in a glass desiccator, in  
 108 which a P<sub>2</sub>O<sub>5</sub> powder were placed as a drying agent, without heating or vacuum. Next, they were manually grinded by  
 109 means of an agate mortar to achieve a fine particle size, in order to perform the next analyses. Finally, the grinded samples  
 110 were analysed by means of XRD patterns, which were recorded in a  $\theta / 2\theta$  X'Pert PANalytical instrument with an  
 111 X'Celerator (Malvern Panalytical Ltd., Malvern, UK). The Cu K $\alpha$  1 ( $\lambda = 1.5403 \text{ \AA}$ ) radiation was provided by a Ge 111  
 112 monochromator, in an angular range ( $^{\circ}2\theta$ ) of 3–70°. This method allowed measurements equivalent to 0.016° angular steps  
 113 for 100 s at each step. The voltage and intensity of the operated X-ray Cu tube were 45 kV and 40 mA, respectively. Semi-  
 114 quantification of Montmorillonite (Sm-di(Al)), Saponite (Sm-tri(Mg)), Sepiolite (Sep), Palygorskite (Plg), Illite (Ilt),  
 115 Quartz (Qtz), Microcline (Mc), Albite (Ab), Calcite (Cal) and Dolomite(Dol) was performed by the Reference Intensity  
 116 Ratio (RIR) method (Zhou et al. 2018; Amonette et al. 1994). The RIR values were based on the previous established semi-  
 117 quantifications (Cuevas et al. 2014) on the basis of the International Centre for Diffraction Data (ICDD) powder diffraction

files (PDF) standards supported in High Score Expert plus © software (vs. 2.1.b 2005), where the RIR values had been set to those of more poorly ordered clay minerals, in order to adjust the semi-quantification to previously known bentonite compositions.

### 2.3. Polycyclic aromatic hydrocarbon analyses

Five grams of wet soil previously sieved to  $\leq 2$  mm was extracted with acetone:hexane (1:1), and analysed using High-Performance Liquid Chromatography–Photodiode Array Detection (HPLC-PDA) as described García-Delgado et al. (2013). The HPLC system was a Waters 2695 separation module coupled with a Waters 996 PDA. The analytical cartridge column was a Supelcosil LCPAH,  $250 \times 3$  mm,  $5 \mu\text{m}$ . The cartridge column was protected by a Supelguard LC-18  $20 \times 3$  mm guard column. The mobile phase was an acetonitrile-water gradient at a flow rate of  $0.5 \text{ mL min}^{-1}$ . The gradient elution program was 0–5 min: 60% acetonitrile and 40% water, then a linear gradient elution from 60% acetonitrile at 5 min to 100% acetonitrile at 15 min, followed by isocratic elution for 10 min. The column run temperature was fixed at  $28^\circ\text{C}$ . The sample injection volume was  $20 \mu\text{L}$ . The chromatograms were monitored at a wavelength of 254 nm and processed by Empower software (Waters, Milford, Massachusetts, USA). The 16 US EPA priority PAHs were analysed: naphthalene (Naph), acenaphthylene (Acy), acenaphthene (Ace), fluorene (Flu), benzo(a)pyrene (BaP), chrysene (Chy), phenanthrene (Phe), anthracene (Ant), fluoranthene (Fla), pyrene (Pyr), benzo(a)fluoranthene (BaA), benzo(b)fluoranthene (BbF), benzo(k)fluoranthene (BkF), dibenzo(a,h)anthracene (DBhaA), benzo(g,h,i)perylene (BgHiP) and indeno(123-cd)pyrene (IcdP). The percentage of recovery of each PAH with respect to the certified reference material CRM141 ranged from 51% to 128% (García-Delgado et al., 2013, 2016) The precision was satisfactory in both previous works with % RSD < 20, except for 2-ring PAHs, the most volatile PAHs.

### 2.4. Trace element analyses

Another 25 g for each soil sample was dried in a  $\text{P}_2\text{O}_5$  conditioned desiccator at room temperature, then, the samples were mildly ground using a TEFLON® jar and TEFLON® bar, avoiding the breakage of hard mineral grains. Next, the ground material was sieved through a  $0.125 \text{ mm}$  nylon mesh screen, and then  $0.5 \text{ g}$  of this size particle was subjected to acid digestion in order to analyze trace elements. The acid attack was carried out with purified  $\text{HNO}_3$  in TEFLON® reactors. The digestions were performed in a CEM-VERTEX Mars Model microwave. The procedure was analogue to the US EPA SW 846 Method 3051 (EPA 2007) recommended for the extraction of metals including Al, As, Ba, Cd, Ca, Cr, Co, Cu, Fe, and Pb (Das and Ting 2017). Digestion was conducted at  $175^\circ\text{C}$  with a ramp of 5.5 min while maintaining the temperature during 4.5 min, hereafter it was left to cool at room conditions. The suspension was diluted with MILIQ ultrapure water and filtered (polypropylene membrane; pore size  $0.20 \mu\text{m}$ ). For the trace element determinations, the samples were diluted 10 times with 0.5% v/v  $\text{HNO}_3$  solution. Then, they were subjected to Inductively Coupled Plasma Mass Spectrometry (ICP-MS). The equipment used was the Thermo Scientific™ Element 2™ SF-ICP-MS model of double focus unique collector. The analyses of  $^7\text{Li}$ ,  $^9\text{Be}$ ,  $^{11}\text{B}$ ,  $^{88}\text{Sr}$ ,  $^{89}\text{Y}$ ,  $^{107}\text{Ag}$ ,  $^{111}\text{Cd}$ ,  $^{137}\text{Ba}$ ,  $^{139}\text{La}$ ,  $^{140}\text{Ce}$ ,  $^{205}\text{Tl}$ ,  $^{208}\text{Pb}$ ,  $^{209}\text{Bi}$ ,  $^{232}\text{Th}$ ,  $^{238}\text{U}$  were performed in a low-resolution mode ( $m / m 300$ ). In order to reduce polyatomic interference, the resolution was increased as follows: a medium-resolution ( $m / m 2000$ ) was utilized to determine  $^{27}\text{Al}$ ,  $^{45}\text{Sc}$ ,  $^{51}\text{V}$ ,  $^{52}\text{Cr}$ ,  $^{55}\text{Mn}$ ,  $^{60}\text{Ni}$ ,  $^{63}\text{Cu}$  and  $^{66}\text{Zn}$ , and a high-resolution mode ( $m / m 10.000$ ) was utilized to determine  $^{75}\text{As}$  and  $^{78}\text{Se}$ . The analyses were carried out with a micro-volume automatic injector (SC-2 DX FAST Autosampler, ESI Inc., Omaha, NE, EE.UU.) and a micro-flux nebulizer PFA in a spray chamber cooled by Peltier, equipped with a sapphire injector tube (ESI Inc., Omaha, NE, EE.UU.).

## 2.5 Statistical analysis

In order to study the results of chemical analyses, IBM® SPSS® statistics were utilized. Pearson's correlation coefficient was used to measure the strength of relationships between pairs of variables. The significance level (p-value) was fixed at  $\leq 0.05$ , and coefficients higher than 0.60 were considered as being a medium–strong association. Due to the relatively reduced number of samples, spatial distribution maps were plotted to visualize qualitative tendencies not showed by the statistical tools. Therefore, lattice points (taking into account their coordinates and altitudes) of the area were selected, forming a representative grid of the sampling zone. Next, the grid was interpolated using Surfer Golden Software® to create a contour topographic map. Finally, another new contour line map was overlaid on the topographic map in order to display the concentrations of each metal or PAHs variable present in each sample.

## 3. Results

### 3.1 Mineralogical composition

The XRD patterns of the soil samples are shown in Fig 2. They are plotted in accordance with the distance to the tire fire. The samples Sp2, Sp9, Sp10, Sp11 and Sp14 are highlighted by the presence of broad reflections in a  $\sim 14$  Å, which is characteristic of the Sm group. Within this group, Sm di- and tri-octahedral are present attending to  $d(060)$  values (1.50 Å and 1.52 Å respectively). On the other hand, Sp3, Sp4, Sp5 and Sp6 showed a high intensity in the Cal and/or Qtz reflections (3.035 Å and 3.34 Å) which makes the visualization of the other minerals difficult, since they are overlapped, with broad characteristic reflections of Sm-di(Al). Similarly, Sp7 and Sp8 present Cal in addition to Sm-tri (Mg) and Sm-di(Al), respectively. In addition, Ilt (10.0 Å) and feldspars (3.21–3.18 Å) were identified. Finally, it is worth mentioning the  $d(110)$  value from Sep (12.2 Å) and Plg (10.4 Å), present in Sp13 and Sp12, respectively. The semi-quantitative mineralogical composition of the samples is presented in Table 1.

**Table 1** Mineralogical composition of the samples (wt. %) and assigned reference intensity ratio (RIR) values

| Mineral    | RIR | Sp1 | Sp2  | Sp3 | Sp4  | Sp5 | Sp6 | Sp7 | Sp8 | Sp9  | Sp10 | Sp11 | Sp12 | Sp13 | Sp14 |
|------------|-----|-----|------|-----|------|-----|-----|-----|-----|------|------|------|------|------|------|
| Sm-di(Al)  | 0.2 | < 1 | 23   | 9   | 10   | 1   | <1  | 4   | 1   | 9    | 9    | 14   | 2    | 6    | 10   |
| Sm-tri(Mg) | 0.3 | < 1 | 41   | 2   | 3    | +   | < 1 | 3   | 1   | 8    | 7    | 14   | 2    | 6    | 9    |
| Sep        | 1   | < 1 | 4    | < 1 | < 1  | +   | < 1 | < 1 | < 1 | < 1  | < 1  | 1    | 2    | 7    | 1    |
| Plg        | 1   | < 1 | < 1  | < 1 | 2    | +   | 1   | 1   | < 1 | 2    | 2    | 1    | 4    | 5    | 2    |
| Ilt        | 2   | 1   | 11   | 4   | 3    | +   | 3   | 1   | 5   | 1    | 1    | 3    | 10   | 1    | 2    |
| Qtz        | 3   | 71  | 12   | 21  | 15   | +   | 44  | 23  | 34  | 16   | 17   | 3    | 13   | 9    | 17   |
| Mc         | 1   | 18  | 6    | 3   | 2    | +   | 2   | 7   | 9   | 1    | 2    | 1    | 1    | < 1  | 7    |
| Ab         | 0.6 | 9   | 3    | 4   | 5    | +   | 1   | 4   | 7   | 1    | 1    | 1    | 1    | 29   | 4    |
| Cal        | 1   | 2   | +    | 55  | 58   | 97  | 43  | 57  | 42  | 53   | 50   | 59   | 64   | 37   | 39   |
| Dol        | 2.5 | +   | +    | 1   | 3    | +   | 5   | < 1 | 0.1 | 10   | 11   | 3    | 1    | 0    | 9    |
| Σclay min  |     | 3   | 79.5 | 16  | 18.5 | 1.4 | 5.5 | 9.5 | 8   | 20.5 | 19   | 25   | 33   | 25   | 24   |

(+): possible presence. Σclay min: summation of clay minerals (Sm+Sep+Plg+Ilt)

### 3.2. Polycyclic aromatic hydrocarbons

The PAH concentrations for each sample are shown in Table 2. The first column showed the Reference Generic Levels (RGL) established by Spanish legislation (Bulletin 2005) (notice that Phe and BghiP have not been assigned RGL).

With the exception of Sp3, Sp6 and Sp7, all samples presented at least one PAH exceeding the threshold level. A special mention should be made regarding 5 fused-ring PAHs: BaP reaches more than 50 times the RGL (Sp2) and DBhaA is close to exceeding the RGL by more than 10 times (Sp1, Sp2) and by 12 times (Sp4). With regard to the distribution of PAHs present in each sample: Sp1, Sp7, Sp9, Sp11 presented high percentage of Pyr (from 85% to 93%); Sp4, Sp5, Sp12, Sp14 showed percentage of Ace ranging from 85% and 99%; Sp13 presented more heterogeneous presence of PAHs with the predominance of Ace (44%) followed by Naph (30%), Acy (17%) and Pyr (7%); Sp2 obtained ~40% of Acy, ~15% of Naph and ~14% of BaP; Sp6 presented 39% of Chy, ~26% of BbF and ~29% of BaA; finally Sp3 presented ~42% of Naph, ~30% of BghiP, ~11% of Pyr and ~7% of IcdP and BaA.

**Table 2** Concentrations of polycyclic aromatic hydrocarbons (mg/Kg)

| PAHs   | RGL* | Sp1    | Sp2    | Sp3    | Sp4    | Sp5    | Sp6    | Sp7    | **Sp9  | Sp11   | Sp12   | Sp13   | Sp14   |
|--------|------|--------|--------|--------|--------|--------|--------|--------|--------|--------|--------|--------|--------|
| Naph   | 1    | <0.001 | 1.11   | 0.56   | <0.001 | <0.001 | <0.001 | <0.001 | <0.001 | <0.001 | <0.001 | 1.97   | <0.001 |
| Acy    | 6    | <0.006 | 3      | <0.006 | <0.006 | <0.006 | <0.006 | <0.006 | <0.006 | 1.14   | <0.006 | 1.13   | <0.006 |
| Ace    | 1    | <0.003 | 0.19   | <0.003 | 4.29   | 3.38   | <0.003 | <0.003 | <0.003 | <0.003 | 3.18   | 2.91   | 1.58   |
| Flu    | 5    | <0.001 | 0.23   | <0.001 | <0.001 | 0.16   | <0.001 | <0.001 | 0.2    | <0.001 | 0.04   | <0.001 | <0.001 |
| Phe    |      | <0.001 | 0.1    | <0.001 | <0.001 | <0.001 | <0.001 | <0.001 | <0.001 | 0.08   | <0.001 | <0.001 | <0.001 |
| Ant    | 45   | <0.001 | 0.24   | <0.001 | <0.001 | <0.001 | <0.001 | <0.001 | <0.001 | <0.001 | <0.001 | <0.001 | <0.001 |
| Fla    | 8    | 0.91   | 0.33   | <0.001 | 0.13   | 0.22   | <0.001 | 0.03   | <0.001 | <0.001 | <0.001 | <0.001 | <0.001 |
| Pyr    | 6    | 11.72  | 0.31   | 0.14   | 0.1    | <0.001 | <0.001 | 0.3    | 2.94   | 19.91  | <0.001 | 0.48   | <0.001 |
| BaA    | 0.2  | 0.14   | <0.001 | 0.1    | <0.001 | <0.001 | 0.09   | <0.001 | <0.001 | <0.001 | <0.001 | <0.001 | <0.001 |
| Chy    | 20   | <0.003 | 0.12   | <0.003 | 0.02   | <0.003 | 0.12   | <0.003 | <0.003 | <0.003 | <0.003 | <0.003 | <0.003 |
| BbF    | 0.2  | <0.001 | 0.24   | <0.001 | <0.001 | <0.001 | 0.08   | <0.001 | <0.001 | <0.001 | 0.05   | 0.13   | <0.001 |
| BkF    | 2    | <0.001 | 0.23   | <0.001 | <0.001 | <0.001 | <0.001 | <0.001 | <0.001 | <0.001 | <0.001 | <0.001 | <0.001 |
| BaP    | 0.02 | 0.05   | 1.08   | <0.001 | <0.001 | <0.001 | <0.001 | <0.001 | <0.001 | 0.08   | <0.001 | <0.001 | <0.001 |
| DBhaA  | 0.03 | 0.28   | 0.27   | <0.001 | 0.5    | <0.001 | <0.001 | <0.001 | <0.001 | 0.05   | <0.001 | <0.001 | <0.001 |
| BghiP  | -    | 0.14   | <0.001 | 0.4    | <0.001 | <0.001 | <0.001 | <0.001 | <0.001 | <0.001 | <0.001 | <0.001 | <0.001 |
| IcdP   | 0.3  | 0.04   | <0.001 | 0.1    | <0.001 | <0.001 | <0.001 | <0.001 | <0.001 | <0.001 | <0.001 | 0.04   | <0.001 |
| Σ PAHs |      | 13.28  | 7.45   | 1.3    | 5.04   | 3.76   | 0.29   | 0.33   | 3.14   | 21.26  | 3.27   | 6.66   | 1.58   |

\*Reference General Levels (RGL) of soils with no industrial or urban use. \*\* Sp8 and Sp10 did not show significant results and they have been omitted.

Σ PAHs: summation of total PAHs. Limits of detection according to García-Delgado et al. (2013).

Pearson's correlation coefficients between mineralogy and PAHs are shown in Table 3. Sm-di(Al), Sm tri(Mg) and It presented strong positive correlations to several types of 3- and 5,6-ring PAHs while Sep presented high affinity for

199 Naph (2-rings PAH). In addition, Cal only showed negative correlations with Fla, BkF and BaP. Concerning distance to  
200 tire fire and  $\Sigma$  PAHs concentrations, a negative correlation was observed ( $r = -0.60$ ;  $p\text{-value} \leq 0.05$ ). However, the  
201 distribution map showed that  $\Sigma$  PAHs concentrations increases are related to the tire fire proximity related to samples  
202 rich in clay minerals, Sp11, 12 and 13; and also Sp2, rich in clay minerals and also near a main road. (Table 2, Fig 1 and  
203 Fig. 3).

204

205 **Table 3** Significant Pearson's correlation coefficient ( $r$ ) between mineralogical composition and PAHs

| *PAHs | Sm-di(Al) | Sm-tri(Mg) | Sep     | Illt    | Qtz    | Mc      | Ab      | Cal     | Dol    | $\Sigma$ clay min |
|-------|-----------|------------|---------|---------|--------|---------|---------|---------|--------|-------------------|
| Naph  | -         | -          | 0.95*** | -       | -      | -       | -       | -       | 0.68** | -                 |
| Acy   | 0.75**    | 0.94***    | 0.65*   | 0.80**  | -      | -       | -       | -       | -      | 0.91***           |
| Ace   | 0.82***   | 0.96***    | 0.65*   | 0.71**  | -      | -       | -       | -       | -      | 0.90***           |
| Flu   | 0.74**    | 0.65*      | -       | 0.64*   | -      | -       | -       | -       | -      | 0.69**            |
| Phe   | 0.75**    | 0.85**     | -       | 0.77**  | -      | -       | -       | -       | -      | 0.82***           |
| Ant   | 0.82***   | 0.96***    | -       | 0.91*** | -      | -       | -       | -       | -      | 0.93***           |
| Fla   | -         | -          | -       | -       | 0.75** | 0.87*** | 0.84*** | -0.73** | -      | -                 |
| Pyr   | -         | -          | -       | -       | -      | -       | -       | -       | -      | -                 |
| BaA   | -         | -          | -       | -       | 0.68*  | -       | -       | -       | -      | -                 |
| Chr   | -         | -          | -       | 0.73**  | -      | -       | -       | -       | -      | -                 |
| BbF   | -         | 0.78**     | 0.76**  | 0.71**  | -      | -       | -       | -       | -      | 0.76**            |
| BkF   | 0.81***   | 0.96***    | -       | 0.91*** | -      | -       | -       | -0.58*  | -      | 0.93***           |
| BaP   | 0.82***   | 0.96***    | -       | 0.91*** | -      | -       | -       | -0.59*  | -      | 0.94***           |
| DBhaA | -         | -          | -       | -       | -      | -       | 0.62*   | -       | -      | -                 |

206 \*  $p \leq 0.05$ ; \*\*  $p \leq 0.010$ . \*\*\*  $p \leq 0.001$ ; only clay minerals that present significant correlation coefficients have been included

207

### 208 3.3. Trace elements

209 In relation to the trace elements, 25 metals were registered (Table S1), of which 14 have assigned RGL (Fig. 4). None  
210 of the metals surpassed the threshold level by more than 100 times, therefore according to Spanish legislation, the soil is  
211 not considered to be polluted. However, As exceeded the RGL in all samples and in Sp14 the RGL is multiplied fourfold,  
212 while the other samples (with the exception of Sp3) exceed the limit by more than double. Another metal that presents  
213 punctual high values is Cu, which appears in samples close to the tire fire (Sp12, Sp14). Notice that in comparison with  
214 the rest of the samples, these two (As and Cu) present a notable increment in comparison with the other metals. Zn also  
215 present a notable increase in Sp14 comparing to the other sample points, but did not reach the RGL. Correlation analyses  
216 of trace element concentrations and distance to the tire fire showed remarkable correlation coefficients for Th and U, which  
217 present significant 0.63 and 0.66 coefficients, respectively. With regard to the rest of the metals, there were no correlations,  
218 even taking into account the road as a focus of emissions. On the other hand, Sm-di(Al), Sm-tri(Mg) and Illt presented high  
219 affinity for Li, Y, Ba, La, Ce, Th, U, Al, Sc and Cr (Table 4). Finally, Cal presented negative correlation coefficients with  
220 metals and one positive correlation with U.



221

222

**Table 4** Significant Pearson's correlation coefficient (*r*) between mineralogical composition and trace elements

| Trace elements | Sm-di(Al) | Sm-tri(Mg) | Ilt     | Qtz    | Mc     | Ab    | Cal     | Σclay min |
|----------------|-----------|------------|---------|--------|--------|-------|---------|-----------|
| Li             | 0.90***   | 0.87***    | 0.77**  |        | -      | -     |         | 0.87**    |
| Be             | -         | -          |         | -      | -      | -     | -       | -         |
| B              | -         | -          |         | 0.72*  | 0.75** | 0.64* | -0.72*- | -         |
| Sr             | -         | -          | -       |        | -      | -     | -       | -         |
| Y              | 0.69*     | 0.64*      | 0.67*-  | -      | -      | -     | -0.62*  | 0.63*     |
| Ag             | -         | -          |         | 0.72*  | 0.79** | 0.68* | -       | -         |
| Cd             | -         | -          |         | 0.73*  | 0.79** | 0.68* | -       | -         |
| Ba             | -         | -          | 0.68*   | -      | -      | -     |         | 0.62*-    |
| La             | 0.78**    | 0.74**     | 0.75**  | -      | -      | -     | -0.69*  | 0.74**    |
| Ce             | 0.81**    | 0.79**     | 0.76**  | -      | -      | -     | -0.65*  | 0.79**    |
| Tl             | -         | -          |         | 0.73** | 0.80** | 0.71* | -       | -         |
| Bi             | -         | -          |         | 0.71** | 0.81** | 0.67* | -0.61*  | -         |
| Th             | 0.72*     | 0.77**     | 0.76**  | -      |        | -     | -0.76** | 0.74**    |
| U              | 0.75**    | 0.88***    | 0.92*** | -      |        | -     | 0.67*   | 0.84***   |
| Al             | 0.65*     | 0.61**     | -       | -      |        | -     |         | 0.63*     |
| Sc             | 0.72*     | 0.73**     | 0.70*   | -      |        | -     | -0.61*  | 0.72*     |
| V              | -         | 0.68*      | -       | -      |        | -     | -       | 0.68*     |
| Cr             | -         | 0.62*      | -       | -      | -      | -     | -       | -         |

223

\*  $p \leq 0.05$ ; \*\*  $p \leq 0.010$ . \*\*\*  $p \leq 0.001$ ; trace elements and clay minerals that present significant correlation coefficients have been included.

224

225

226

227

228

229

Although no significant correlations were found related to the distance to the tire fire, the distribution map showed qualitative tendencies for Al, Se and Zn (Fig. 5). The highest concentration of Zn above mentioning was localized next to tire fire (Sp14), but also next to the road in the case of Al (Fig. 5, points on the left). Al presented also a strong correlation with Sm di(Al) and tri(Mg). The Se distribution presents similar behaviour to Al, but Se did not present any correlation with the position of collected samples. Regarding Zn contour map, its concentration increases to the south of the tire fire, which is according to the westerly direction of the wind registered on the two days previous to the sampling campaign.

230

#### 4. Discussion

231

##### 4.1 Polycyclic aromatic hydrocarbons and clay minerals

232

233

234

235

236

In the present work, the correlation coefficients between Sm, Ilt, Σclay min and PAHs, and the qualitative tendency showed by the distribution map of PAHs, suggest that soils rich in clay minerals are able to adsorb PAHs. The weather conditions could have transported the PAHs and deposited them at several distances, however, only the soils rich in clay minerals could adsorb and hold them. With regard to, Sp2 and Sp11, these samples are rich in Sm, and presented considerable concentrations of BkF, BbF, (Sp2) and Pyr, BaP (Sp2, Sp11), which have been related with the tire fire (Marco

Pandolfi and Vázquez 2016). The proximity of Sp2 to the main road may indicate a different pollution source, although supports the clay minerals suggested behaviour. This fact could explain the lack of correlation between PAHs concentrations and the distance to the tire fire. Nevertheless, the assumption of the PAHs affected by clay content may be taken into account but should be further evaluated on the basis of more data.

Regarding to PAHs distribution, it is not very important the distance between sample points and tire fire. Then, clay minerals should be evaluated as geo-indicators of an air pollution accident. Sm and Ill seems to be able to indicate emissions provided by low and high molecular weight PAHs, according to the correlation with Sm, Ill and  $\Sigma$ clay min present in soil samples. On the other hand, Sep only indicates affinity with the lowest molecular weight PAHs. The reason is based on their structure: Sm and Ill are 2:1 filosilicates with a high surface area and swelling properties, particularly the Sm group. Sm presents hydrophobic sites and large areas which provide good accessibility to planar PAHs, either with a low and high number of rings. Sep is a different 2:1 fibrous filosilicate, presenting channels due to the lack of continuous octahedral sheets, resulting in small dimensions for coupling to high molecular weight PAHs (González-Santamaría et al. 2017).

The origins of PAHs are difficult to ascertain; PAHs are ubiquitous pollutants and several sources can be involved in their presence, including the fuel combustion of vehicles from roads, and villages or industrial activities. In addition, a number of factors are implicated in their distribution, e.g., wind, topography, the temperature reached in the fire, the nature of the generated aromatics or even the method used in the extinction of the fire (Paul M Lemieux et al. 1993). Previous works carried out in relation to the Seseña tire fire did not find correlations with distance either (Escobar-Arnanz et al. 2018; Nadal et al. 2016). With regard to the present work, it can be highlighted that the samples next to the road (Sp2, Sp3, and Sp6) showed the greatest heterogeneity of PAHs, reflecting the influence of vehicle emissions. In contrast, the samples next to the fire (Sp12, Sp13 and Sp14) present high quantities and a predominance of Ace, suggesting its origin from the tire fire. Several works focussing on the characterizations of air pollutants emitted from simulated scrap tire fires also showed that the highest PAH emitted was Ace. (Paul M. Lemieux et al. 2004; Paul M Lemieux et al. 1993; Reisman 1997).

Numerous types of PAH ratios have been proposed to study their origin (Budzinski et al. 1997; Benlahcen et al. 1997; Yang 2000). Based on the % of Naph, Sp3 could have a combustion source, which is due to its location next to the road. However, Sp2 presented both origins: from the tire fire, according to the ratios Phe/Ant < 10 and Fla/Pyr > 1, and from vehicles regarding the % of Naph. In fact, Fla/Pyr ratios close to unit can indicate both sources (Downard et al. 2015).

The smoke plume emitted by tire fire has been proven to contain hazardous PAHs identified as mutagenic (Orecchio et al. 2017), their carcinogenicity is associated with the increase in the number of rings (Saeedi et al. 2012), Pyr and BaP present 4 and 5 fused rings, respectively. Special attention should be paid to BaP, which has been demonstrated as a strong carcinogenic substance (Collins et al. 1991), and a continued monitoring of the area should be performed.

#### 4.2 Trace elements and clay minerals

Although a number of trace and major elements analysed are significantly correlated to clay minerals (Li, Y, Ba, La, Ce, Th, U, Al, Sc and Cr), only Th and U presented correlation to the distance of the tire fire. Li, Y, Ba, La, Ce, Th, U, Al, Sc and Cr did not show this correlation because they were present in the soil and remain adsorbed to clay minerals from

before the accident. Additionally, they did not reach the RGL. On the contrary, As and Cu surpassed the RGL but did not present correlation with clay minerals.

With regard to As, the absence of correlation with clay minerals could be related to their predominantly negative charge-forming anion compounds. Clay minerals presented a predominantly permanent negative surface charge, and they did not have permanent positive surface sites available for anions. However, a certain quantity of As can be retained by means of several mechanisms e.g., chemisorption or indirectly throughout intermediate cations (Goldberg 2002).

As is naturally present, but its increases further than RGL may indicate human-induced activities such as mining, coal burning or pesticides (Garelick et al. 2008). Considering that the sampling was performed in agricultural areas, their anthropogenic source is likely to come from pesticides or fertilizers. In respect to As risks, it is a “non-essential” metal and toxic at low concentrations but based on the total concentrations that may be in error, the speciation of As (III or V) has to be conducted in order to determine the As risk assessment (Akter et al. 2005). Additionally, higher concentrations of As were found in the post-fire situation by Nadal et al. (2016) in the closest populated nuclei.

Although no correlations or tendencies were found between clay minerals and Cu, the high levels present in Sp12 and Sp14 may be associated with the tire fire. Sp12 and Sp14 were close to the tire fire and they were directly exposed to the smoke plume, while the rest of the samples in the fire’s proximity (with the exception of Sp13, rich in clay minerals) showed lower Cu concentrations. This fact is in agreement with the findings of the post-fire studies mentioned above. Cu is present in the tire composition and evidence of an increase linked to the fire was found in deposited dust loadings obtained 10 days after the start of the fire (Artiñano et al. 2017).

Regarding Al, Se and Zn, the trend to increase with the proximity to the fire is according to the wind component and the tendency suggested by the distribution maps. Additionally, in the case of Al and Zn, the combustion of tires produces ash rich in metals such as Zn and Al. On the other hand, ZnO and Al<sub>2</sub>O<sub>3</sub> increases were found in the deposited dust loadings (Artiñano et al. 2017). Al showed a strong correlation with clay minerals, presumably because of its presence as a significant part of their composition, so it is not a conclusive indicator. Despite of the highest concentration of Zn found next to tire fire, Zn did not present any correlation with the clay mineral content. This means that Zn was not migrated in an ionic soluble form susceptible to be adsorbed in clay mineral surfaces.

## 5. Conclusions

This paper quantifies the preliminary impact of a landfill tire fire trying to look for assessing the use of clay minerals present in soil as pollution indicators. The concentrations of PAHs and trace elements were higher than the threshold levels related to samples rich in these minerals. Therefore, the environmental impact of the tire fire was demonstrated by analyzing the pollutants trapped by smectite, illite and the summation of clay minerals. These clay minerals showed positive correlation with PAHs of high and low molecular weight, whereas metals and trace elements, such as As, Zn, Al, and Cu, are more related to the distance to the tire fire or the direction of the smoke plume.

A major finding is that the presence of clay mineral-rich soils determined the detection of air pollutants, showing particularly affinity with PAHs. These results indicate the possibility of using clay minerals as geo-indicators of air

pollution, complementary to current atmospheric and biological analyses. In doing these a more samples and more data will be further analysed in order to have more sounded statistics considering this application of clay minerals.

## 6. Acknowledgments

This work has been economically supported by the Ministry of Economy and Competitiveness of Spain, project AGL2016-78490-R.

## 7. References

- Akhbarizadeh, R., Moore, F., Keshavarzi, B., & Health (2019). Polycyclic aromatic hydrocarbons and potentially toxic elements in seafood from the Persian Gulf: presence, trophic transfer, and chronic intake risk assessment. [journal article]. *Environmental Geochemistry and Health*, <https://doi.org/10.1007/s10653-019-00343-1>
- Akter, K. F., Owens, G., Davey, D. E., & Naidu, R. (2005). Arsenic speciation and toxicity in biological systems. In *Reviews of environmental contamination and toxicology* (pp. 97-149): Springer.
- Amonette, J. E., Zelazny, L. W., & Luxmoore, R. J. (1994). *Quantitative methods in soil mineralogy: proceedings of a symposium sponsored by Division S-9 of the Soil Science Society of America : the symposium was held in San Antonio, Texas on October 23-24, 1990*: Soil Science Society of America.
- Artiñano, B., Gómez-Moreno, F. J., Díaz, E., Amato, F., Pandolfi, M., Alonso-Blanco, E., et al. (2017). Outdoor and indoor particle characterization from a large and uncontrolled combustion of a tire landfill. *Science of The Total Environment*, 593-594, 543-551, <https://doi.org/10.1016/j.scitotenv.2017.03.148>
- Benlahcen, K. T., Chaoui, A., Budzinski, H., Bellocq, J., & Garrigues, P. (1997). Distribution and sources of polycyclic aromatic hydrocarbons in some Mediterranean coastal sediments. *Marine Pollution Bulletin*, 34(5), 298-305, [https://doi.org/10.1016/S0025-326X\(96\)00098-7](https://doi.org/10.1016/S0025-326X(96)00098-7)
- Bergaya, F., & Lagaly, G. (2013). Chapter 1 - General Introduction: Clays, Clay Minerals, and Clay Science. In F. Bergaya, & G. Lagaly (Eds.), *Developments in Clay Science* (Vol. 5, pp. 1-19): Elsevier, [https://doi.org/10.1016/S1572-4352\(05\)01001-9](https://doi.org/10.1016/S1572-4352(05)01001-9)
- Budzinski, H., Jones, I., Bellocq, J., Piérard, C., & Garrigues, P. (1997). Evaluation of sediment contamination by polycyclic aromatic hydrocarbons in the Gironde estuary. *Marine Chemistry*, 58(1), 85-97, [https://doi.org/10.1016/S0304-4203\(97\)00028-5](https://doi.org/10.1016/S0304-4203(97)00028-5)
- Bulletin, O. S. (2005). Royal Decree 9/2005, of 14th January, establishing the list of potentially polluting activities for the land and the criteria and standards for the declaration of contaminated lands. BOE.
- Bustillo, M. A., & Alonso-Zarza, A. M. J. S. G. (2007). Overlapping of pedogenesis and meteoric diagenesis in distal alluvial and shallow lacustrine deposits in the Madrid Miocene Basin, Spain. 198(3-4), 255-271, <https://doi.org/10.1016/j.sedgeo.2006.12.006>
- Churchman, G. J., Gates, W. P., Theng, B. K. G., & Yuan, G. (2006). Chapter 11.1 Clays and Clay Minerals for Pollution Control. In F. Bergaya, B. K. G. Theng, & G. Lagaly (Eds.), *Developments in Clay Science* (Vol. 1, pp. 625-675): Elsevier, [https://doi.org/10.1016/S1572-4352\(05\)01020-2](https://doi.org/10.1016/S1572-4352(05)01020-2)
- Clauer, N., Fallick, A. E., Galán, E., Pozo, M., & Taylor, C. (2012). Varied crystallization conditions for Neogene sepiolite and associated Mg-clays from Madrid Basin (Spain) traced by oxygen and hydrogen isotope geochemistry. *Geochimica et Cosmochimica Acta*, 94, 181-198, <https://doi.org/10.1016/j.gca.2012.07.016>
- Cobas, M., Ferreira, L., Sanromán, M., & Pazos, M. (2014). Assessment of sepiolite as a low-cost adsorbent for phenanthrene and pyrene removal: Kinetic and equilibrium studies. *Journal of Ecological Engineering*, 70, 287-294, <https://doi.org/10.1016/j.ecoleng.2014.06.014>
- Collins, J. F., Brown, J. P., Dawson, S. V., & Marty, M. A. (1991). Risk assessment for benzo[a]pyrene. *Regulatory Toxicology and Pharmacology*, 13(2), 170-184, [https://doi.org/10.1016/0273-2300\(91\)90020-V](https://doi.org/10.1016/0273-2300(91)90020-V)
- Cuevas, J., Fernández, R., Ortega, A. y Ruiz, A.I. (2014). Comparison of alternative bentonites for potential use as buffer and sealing materials in the Swiss concept for radioactive waste disposal. Part 2: Results. *Nagra internal report. Arbeitsbericht NAN 14-65*. 76pp.
- Das, S., & Ting, Y.-P. (2017). Evaluation of Wet Digestion Methods for Quantification of Metal Content in Electronic Scrap Material. *Resources*, 6(4), 64, <https://doi.org/10.3390/resources6040064>

Downard, J., Singh, A., Bullard, R., Jayarathne, T., Rathnayake, C. M., Simmons, D. L., et al. (2015). Uncontrolled combustion of shredded tires in a landfill – Part 1: Characterization of gaseous and particulate emissions. *Atmospheric Environment*, 104, 195-204, <https://doi.org/10.1016/j.atmosenv.2014.12.059>

EPA (2007). SW-846 Test Method 3051A: Microwave Assisted Acid Digestion of Sediments, Sludges, Soils, and Oils. (pp. 30 ): United States Environmental Protection Agency.

Escobar-Arnanz, J., Mekni, S., Blanco, G., Eljarrat, E., Barceló, D., & Ramos, L. (2018). Characterization of organic aromatic compounds in soils affected by an uncontrolled tire landfill fire through the use of comprehensive two-dimensional gas chromatography–time-of-flight mass spectrometry. *Journal of Chromatography A*, 1536, 163-175, <https://doi.org/10.1016/j.chroma.2017.10.044>

FAO, I. W. G. (2015). World reference base for soil resources 2014, update 2015: International soil classification system for naming soils and creating legends for soil maps. *WRB, J World Soil Resources Reports No. 106* (pp. 192).

García-Delgado, C., Yunta, F., & Eymar, E. (2013). Methodology for Polycyclic Aromatic Hydrocarbons Extraction from Either Fresh or Dry Spent Mushroom Compost and Quantification by High-Performance Liquid Chromatography–Photodiode Array Detection. *Communications in Soil Science and Plant Analysis*, 44(1-4), 817-825, <http://dx.doi.org/10.1080/00103624.2013.749439>

García-Delgado, C., Yunta, F., & Eymar, E. (2016). Are physico-chemical soil characteristics key factors to select the polycyclic aromatic hydrocarbons extraction procedure? *International Journal of Environmental Analytical Chemistry* 96(1), 87–100.

Garelick, H., Jones, H., Dybowska, A., & Valsami-Jones, E. (2008). Arsenic Pollution Sources. In *Reviews of Environmental Contamination Volume 197: International Perspectives on Arsenic Pollution and Remediation* (pp. 17-60). New York, NY: Springer New York, [https://doi.org/10.1007/978-0-387-79284-2\\_2](https://doi.org/10.1007/978-0-387-79284-2_2)

Goldberg, S. (2002). Competitive adsorption of arsenate and arsenite on oxides and clay minerals. *Soil Science Society of America Journal*, 66(2), 413-421.

González-Santamaría, D., López, E., Ruiz, A., Fernández, R., Ortega, A., & Cuevas, J. (2017). Adsorption of phenanthrene by stevensite and sepiolite. 52(3), 341-350, <https://doi.org/10.1180/claymin.2017.052.3.05>

Hundal, L. S., Thompson, M. L., Laird, D. A., Carmo, A. M., & technology (2001). Sorption of phenanthrene by reference smectites. *Environmental Science & Technology*, 35(17), 3456-3461, <https://doi.org/10.1021/es001982a>

Lemieux, P. M., Lutes, C. C., & Santoianni, D. A. (2004). Emissions of organic air toxics from open burning: a comprehensive review. *Progress in Energy and Combustion Science*, 30(1), 1-32, <https://doi.org/10.1016/j.pecs.2003.08.001>

Lemieux, P. M., Ryan, J. V., (1993). Characterization of air pollutants emitted from a simulated scrap tire fire. *Journal of the Air & Waste Management Association*, 43(8), 1106-1115, <https://doi.org/10.1080/1073161X.1993.10467189>

JCCM (2016). Información Ambiental. Junta de Castilla-La Mancha. [http://pagina.jccm.es/medioambiente/rvca/incendio\\_sesena.htm](http://pagina.jccm.es/medioambiente/rvca/incendio_sesena.htm) Accessed 1 May 2019.

Pandolfi, M., Alastuey, A., Cabañas, M., Martínez, S., Rebeca, C., Vázquez, L., Artíñano, B., Díaz-Ramiro E., García-Alonso, S. (2016). Muestreo y análisis del polvo respirable depositado en exteriores e interiores del CEIP El Quiñón, Seseña. (pp. 14): Instituto de Diagnóstico Ambiental y Estudios del Agua del Consejo Superior de Investigaciones Científicas (IDAEA-CSIC), y Departamentos de Medio Ambiente y la División de Química del Centro de Investigaciones Energéticas, Medioambientales y Tecnológicas (CIEMAT). [http://pagina.jccm.es/medioambiente/rvca/incendio/Informe\\_CSIC\\_CIEMAT\\_30\\_05\\_2016.pdf](http://pagina.jccm.es/medioambiente/rvca/incendio/Informe_CSIC_CIEMAT_30_05_2016.pdf) Accessed 1 May 2019.

MeteoValdemoro (2016). Datos climatológicos Valdemoro. <http://www.meteovaldemoro.es/NOAA2016.TXT>. Accessed 19 June 2019.

Nadal, M., Rovira, J., Diaz-Ferrero, J., Schuhmacher, M., & Domingo, J. L. (2016). Human exposure to environmental pollutants after a tire landfill fire in Spain: Health risks. *Environ Int*, 97, 37-44, <http://dx.doi.org/10.1016/j.envint.2016.10.016>

Orecchio, S., Fiore, M., Barreca, S., & Vara, G. (2017). Volatile Profiles of Emissions from Different Activities Analyzed Using Canister Samplers and Gas Chromatography–Mass Spectrometry (GC/MS) Analysis: A Case Study. *Environmental Research and Public Health*, 14(2), 195, <https://doi.org/10.3390/ijerph14020195>

Reisman, J. (1997). Air emissions from scrap tire combustion. U.S. Environmental Protection Agency, Washington, D.C.

- Saeedi, M., Li, L. Y., & Zadeh, S. M. (2012). Heavy metals and polycyclic aromatic hydrocarbons: pollution and ecological risk assessment in street dust of Tehran. *Journal of Hazardous Materials*, 227, 9-17, <http://dx.doi.org/10.1016/j.jhazmat.2012.04.047>
- Seidelt, S., Müller-Hagedorn, M., Bockhorn, H. (2006). Description of tire pyrolysis by thermal degradation behaviour of main components. *Journal of Analytical and Applied Pyrolysis*, 75(1), 11-18, <https://doi.org/10.1016/j.jaap.2005.03.002>
- Steer, P. J., Tashiro, C. H., Mcillveen, W. D., Clement, R. E. (1995). PCDD and PCDF in air, soil, vegetation and oily runoff from a tire fire. *Water, Air, & Soil Pollution*, 82(3), 659-674, <https://doi.org/10.1007/BF00479418>
- Stewart, A., & Hursthouse, A.. (2018). Environment and human health: the challenge of uncertainty in risk assessment. *Geosciences*, 8(1), 24, <https://doi.org/10.3390/geosciences8010024>
- Swift, R., & McLaren, R. (1991). Micronutrient adsorption by soils and soil colloids. In *Interactions at the Soil Colloid—Soil Solution Interface* (pp. 257-292): Springer, [https://doi.org/10.1007/978-94-017-1909-4\\_9](https://doi.org/10.1007/978-94-017-1909-4_9)
- Swyngedouw, C., & Crépin, J. M. (2008). CHAPTER TWO - SAMPLING METHODS FOR SITE CHARACTERIZATION. In B. De Vivo, H. E. Belkin, & A. Lima (Eds.), *Environmental Geochemistry* (pp. 13-27). Amsterdam: Elsevier, <https://doi.org/10.1016/B978-0-444-53159-9.00002-4>
- USDA (2014). Keys to soil taxonomy. (pp. 372): Soil Survey Staff.
- Volzone, C. (2007). Retention of pollutant gases: Comparison between clay minerals and their modified products. *Applied Clay Science*, 36(1), 191-196, <https://doi.org/10.1016/j.clay.2006.06.013>
- Wang, Z., Li, K., Lambert, P., & Yang, C. (2007). Identification, characterization and quantitation of pyrogenic polycyclic aromatic hydrocarbons and other organic compounds in tire fire products. *Journal of Chromatography A*, 1139(1), 14-26, <https://doi.org/10.1016/j.chroma.2006.10.085>
- Yang, G.-P. (2000). Polycyclic aromatic hydrocarbons in the sediments of the South China Sea. *Environmental Pollution*, 108(2), 163-171, [https://doi.org/10.1016/S0269-7491\(99\)00245-6](https://doi.org/10.1016/S0269-7491(99)00245-6)
- Zhou, X., Liu, D., Bu, H., Deng, L., Liu, H., Yuan, P., et al. (2018). XRD-based quantitative analysis of clay minerals using reference intensity ratios, mineral intensity factors, Rietveld, and full pattern summation methods: A critical review. *Solid Earth Sciences*, 3(1), 16-29, <https://doi.org/10.1016/j.sesci.2017.12.002>

## List of Captions

**Fig. 1** Sampling area

**Fig. 2** X-ray diffraction (XRD) powder patterns ordered from top (furthest sample from tire fire) to bottom (nearest sample to tire landfill). Montmorillonite (Sm-di), Saponite (Sm-tri), Sepiolite (Sep), Palygorskite (Plg), Illite (Ilt), Quartz (Qtz), Microcline and Albite (are refereed as Fds), Calcite (Cal) and Dolomite (Dol)

**Fig. 3** Contour map of the distribution of total PAHs. The X- and Y-axes represents the UTM coordinates. Left scale corresponds to total PAHs (mg/kg) while the right scale corresponds to altitude (m). Numbers associated with contour lines represent the mg/Kg of the summation of PAHs. The black diamonds represents the sampling points

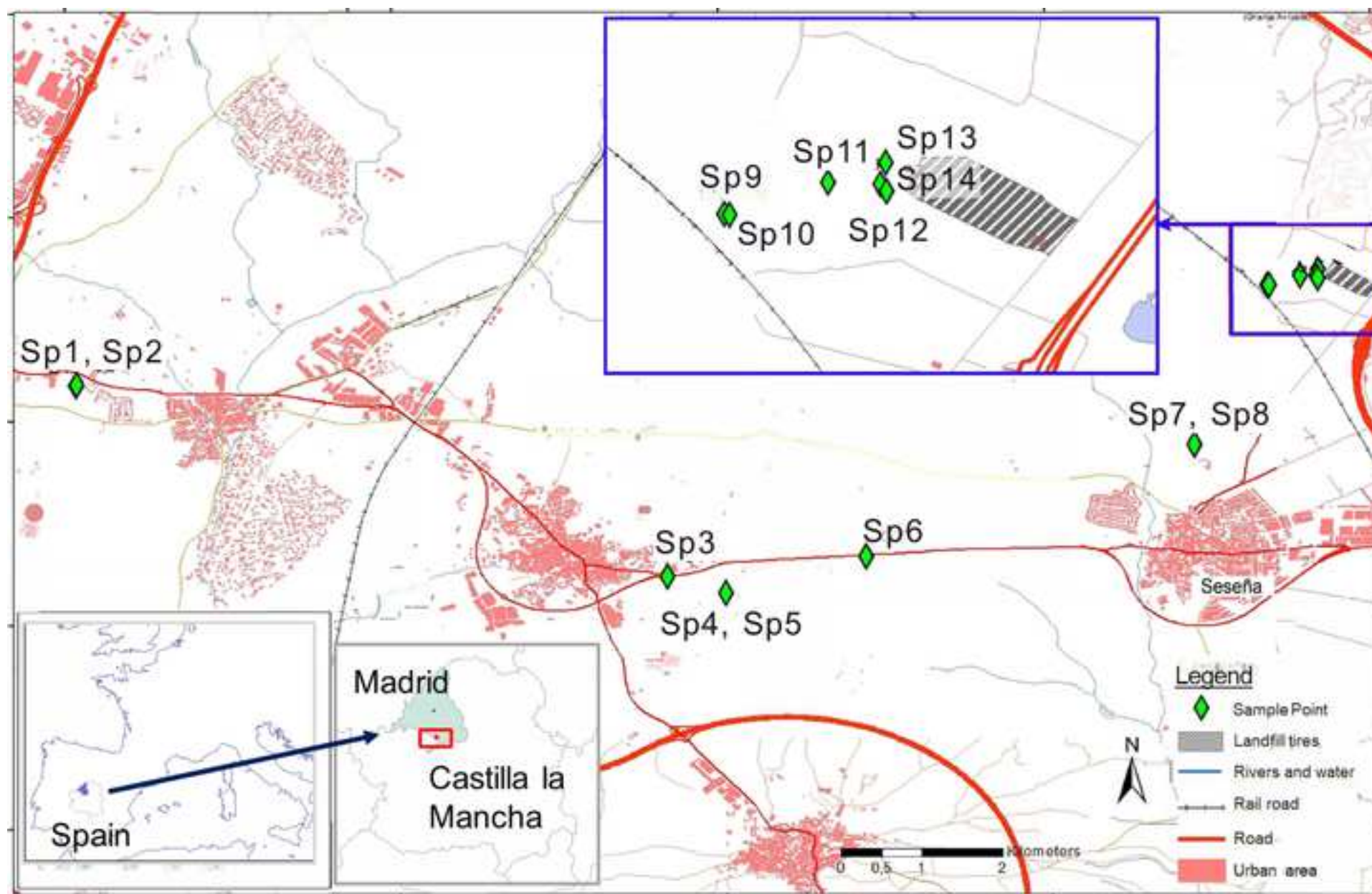
**Fig. 4** Y-Axes represent the Reference General Levels (RGL) of soils with no industrial or urban use. RGL are normalized to 100% for a clearer comparison

**Fig. 5** Contour map of the distribution of Al, Se and Zn. The X- and Y-axis represent the UTM coordinates. On the left scales is depicted the concentration of the metals (mg/kg), while right scales corresponds to altitude (m). Notice that contour lines are have been associated with the concentration of metals (mg/Kg). Black diamonds represent the sampling points





Figure 1





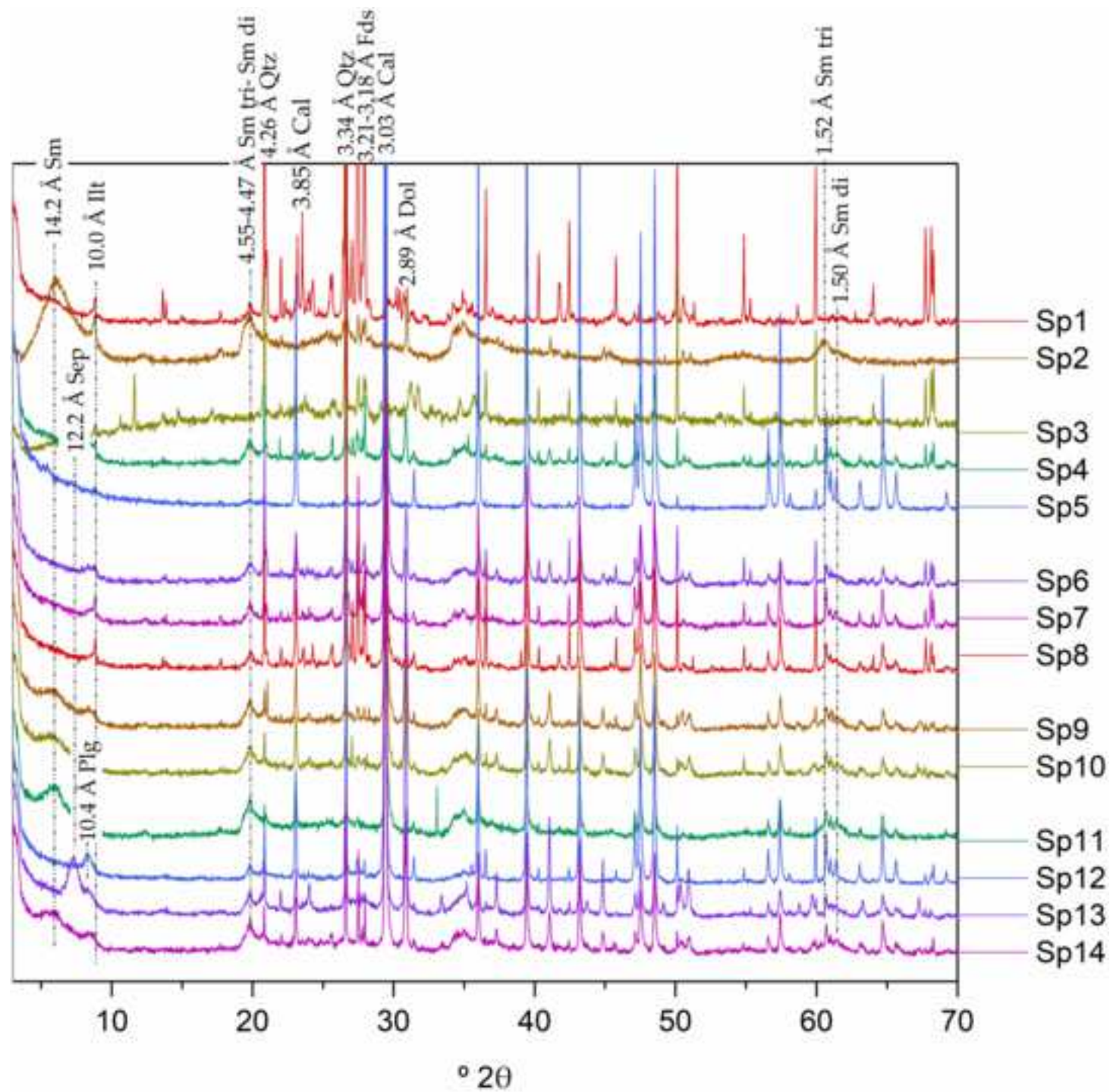


Figure 3

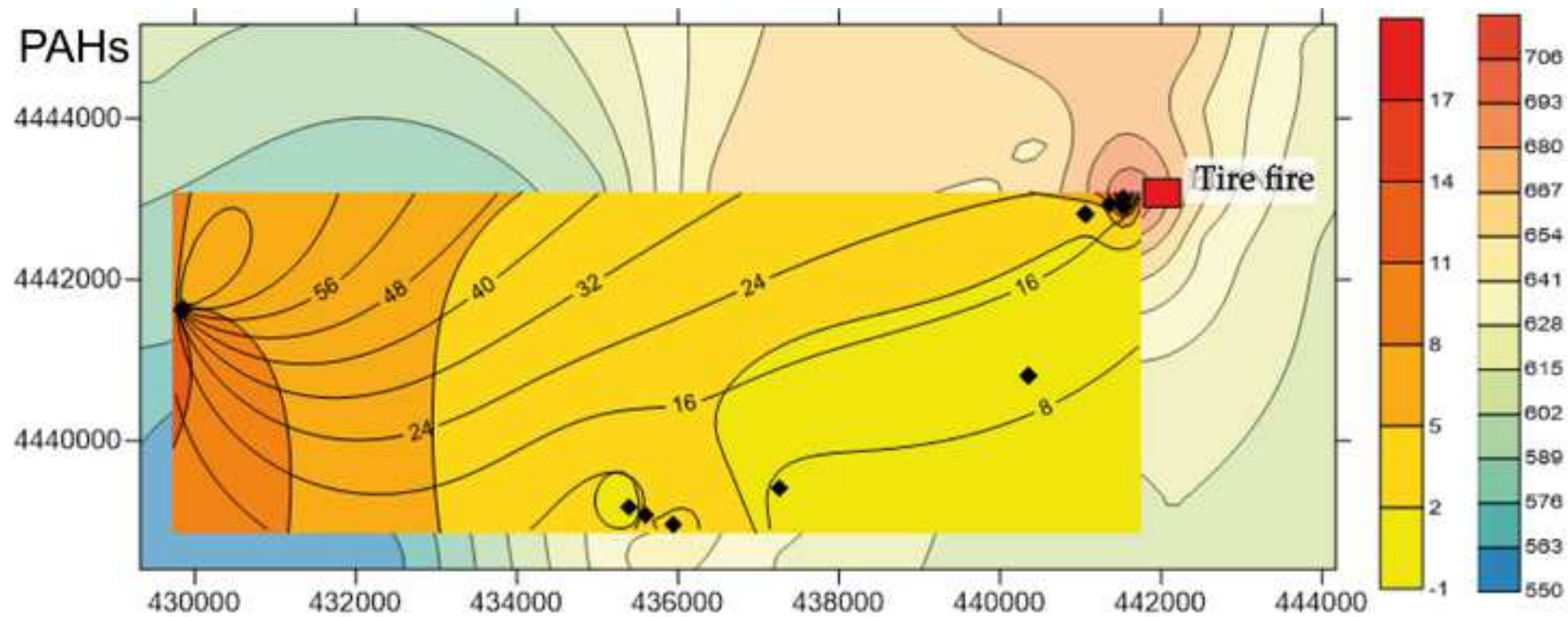


Figure 4

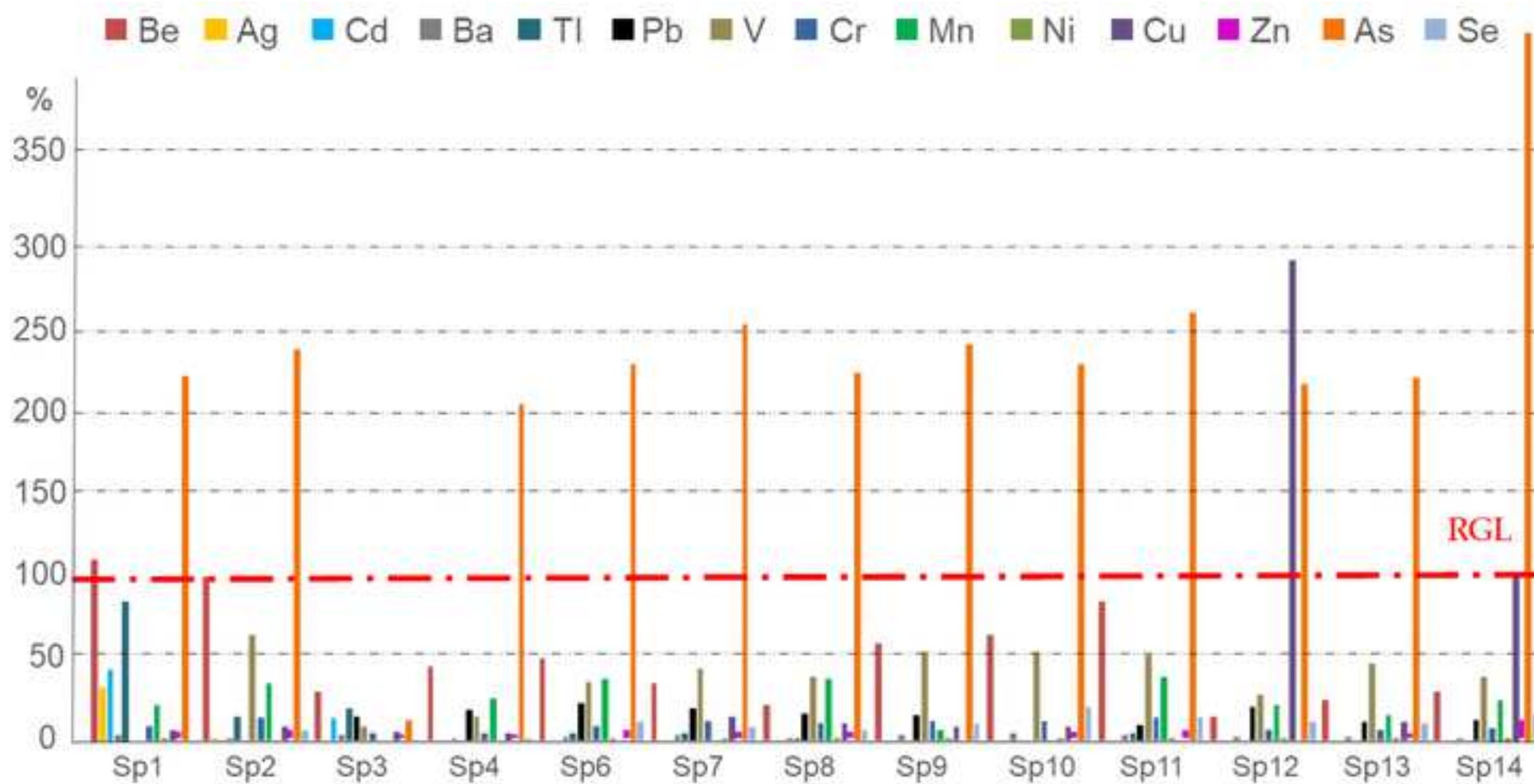
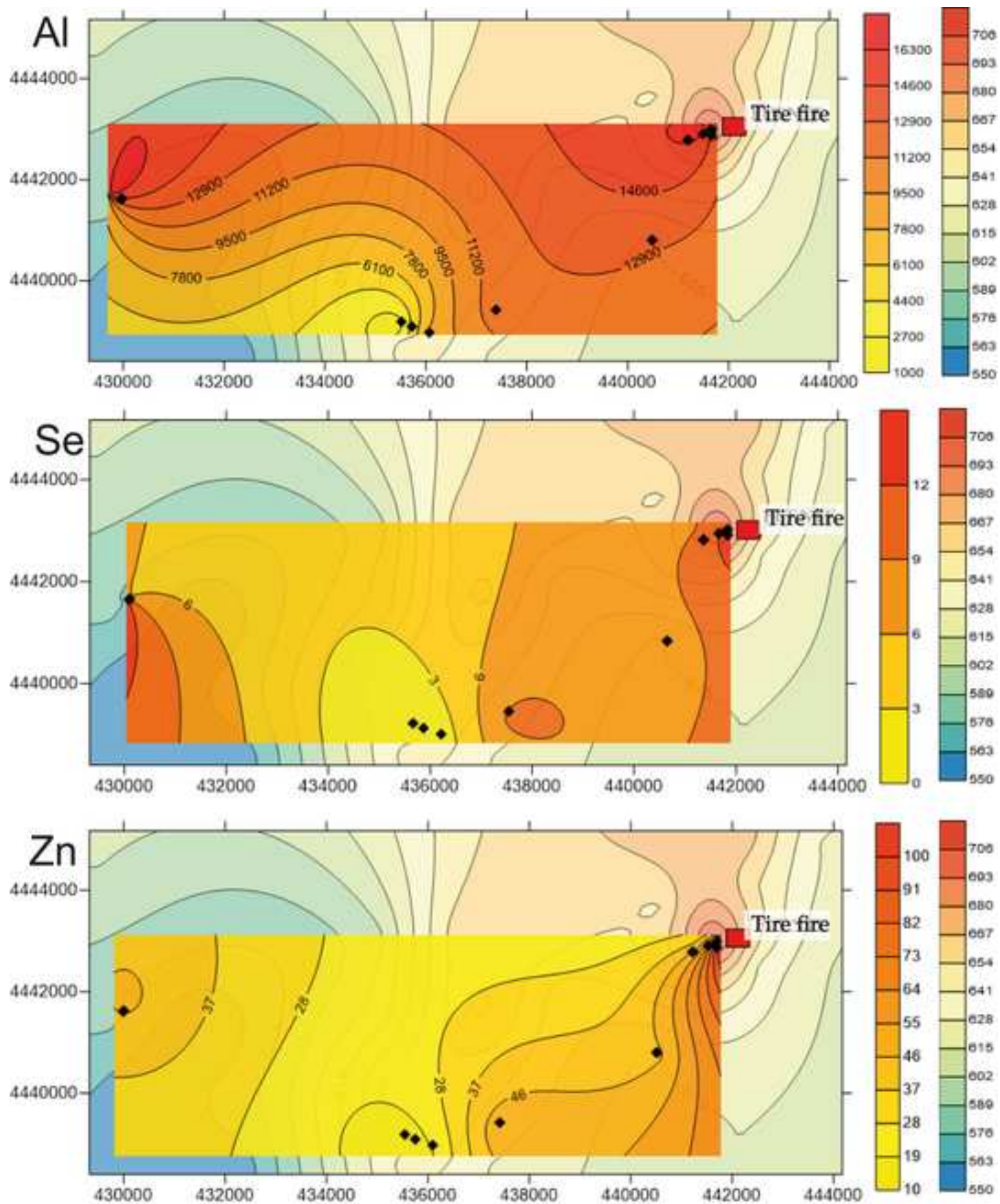
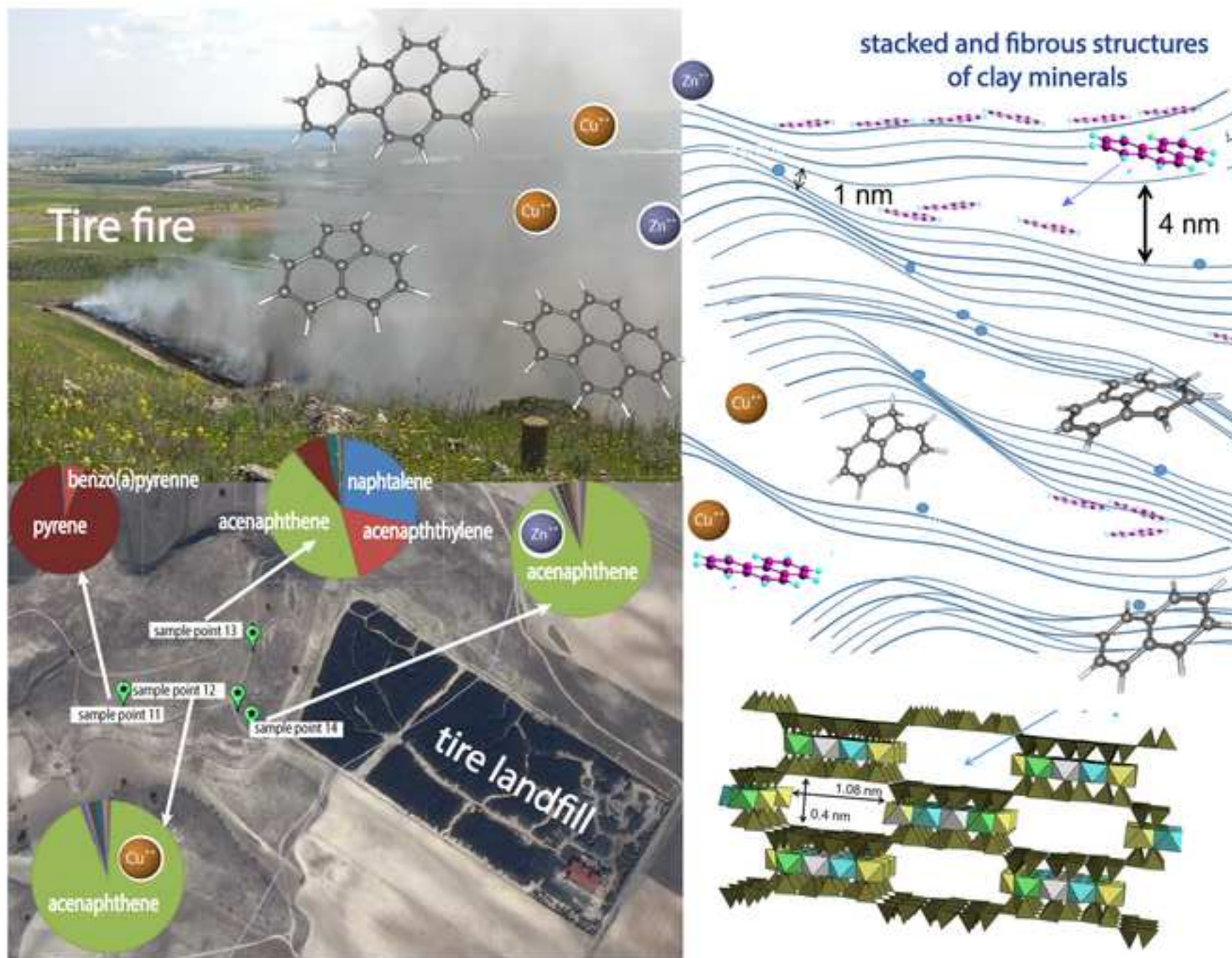




Figure 5

[Click here to download Figure Fig 5.tif](#)





tire fire → clay minerals-adsorption → air pollution geo-indicators

**Table 1** Mineralogical composition of the samples (wt. %) and assigned reference intensity ratio (RIR) values

| Mineral   | RIR | Sp1 | Sp2 | Sp3 | Sp4 | Sp5 | Sp6 | Sp7 | Sp8 | Sp9 | Sp10 | Sp11 | Sp12 | Sp13 | Sp14 |
|-----------|-----|-----|-----|-----|-----|-----|-----|-----|-----|-----|------|------|------|------|------|
| Sm-di(Al) | 0   | < 1 | 23  | 9   | 10  | 1   | <1  | 4   | 1   | 9   | 9    | 14   | 2    | 6    | 10   |
| Sm-tr(Mg) | 0   | < 1 | 41  | 2   | 3   | +   | < 1 | 3   | 1   | 8   | 7    | 14   | 2    | 6    | 9    |
| Sep       | 1   | < 1 | 4   | < 1 | < 1 | +   | < 1 | < 1 | < 1 | < 1 | < 1  | 1    | 2    | 7    | 1    |
| Plg       | 1   | <1  | <1  | <1  | 2   | +   | 1   | 1   | <1  | 2   | 2    | 1    | 4    | 5    | 2    |
| Illt      | 2   | 1   | 11  | 4   | 3   | +   | 3   | 1   | 5   | 1   | 1    | 3    | 10   | 1    | 2    |
| Qtz       | 3   | 71  | 12  | 21  | 15  | +   | 44  | 23  | 34  | 16  | 17   | 3    | 13   | 9    | 17   |
| Mc        | 1   | 18  | 6   | 3   | 2   | +   | 2   | 7   | 9   | 1   | 2    | 1    | 1    | <1   | 7    |
| Ab        | 1   | 9   | 3   | 4   | 5   | +   | 1   | 4   | 7   | 1   | 1    | 1    | 1    | 29   | 4    |
| Cal       | 1   | 2   | +   | 55  | 58  | 97  | 43  | 57  | 42  | 53  | 50   | 59   | 64   | 37   | 39   |
| Dol       | 3   | +   | +   | 1   | 3   | +   | 5   | <1  | 0   | 10  | 11   | 3    | 1    | 0    | 9    |
| Σclay min |     | 1   | 79  | 15  | 18  | 1   | 4   | 9   | 7   | 20  | 19   | 33   | 20   | 25   | 24   |

(+): possible presence. Σclay min: summation of clay minerals (Sm+Sep+Plg+Illt).



| Table 2 Concentrations of polycyclic aromatic hydrocarbons (mg/Kg) |      |        |        |        |        |        |        |        |        |        |        |        |        |
|--|------|--------|--------|--------|--------|--------|--------|--------|--------|--------|--------|--------|--------|
| PAHs   | RGL* | Sp1    | Sp2    | Sp3    | Sp4    | Sp5    | Sp6    | Sp7    | **Sp9  | Sp11   | Sp12   | Sp13   | Sp14   |
| Naph   | 1    | <0.001 | 1.11   | 0.56   | <0.001 | <0.001 | <0.001 | <0.001 | <0.001 | <0.001 | <0.001 | 1.97   | <0.001 |
| Acy  | 6    | <0.006 | 3      | <0.006 | <0.006 | <0.006 | <0.006 | <0.006 | <0.006 | 1.14   | <0.006 | 1.13   | <0.006 |
| Ace  | 1    | <0.003 | 0.19   | <0.003 | 4.29   | 3.38   | <0.003 | <0.003 | <0.003 | <0.003 | 3.18   | 2.91   | 1.58   |
| Flu  | 5    | <0.001 | 0.23   | <0.001 | <0.001 | 0.16   | <0.001 | <0.001 | 0.2    | <0.001 | 0.04   | <0.001 | <0.001 |
| Phe  | -    | <0.001 | 0.1    | <0.001 | <0.001 | <0.001 | <0.001 | <0.001 | <0.001 | 0.08   | <0.001 | <0.001 | <0.001 |
| Ant  | 45   | <0.001 | 0.24   | <0.001 | <0.001 | <0.001 | <0.001 | <0.001 | <0.001 | <0.001 | <0.001 | <0.001 | <0.001 |
| Fla  | 8    | 0.91   | 0.33   | <0.001 | 0.13   | 0.22   | <0.001 | 0.03   | <0.001 | <0.001 | <0.001 | <0.001 | <0.001 |
| Pyr  | 6    | 11.72  | 0.31   | 0.14   | 0.1    | <0.001 | <0.001 | 0.3    | 2.94   | 19.91  | <0.001 | 0.48   | <0.001 |
| BaA  | 0.2  | 0.14   | <0.001 | 0.1    | <0.001 | <0.001 | 0.09   | <0.001 | <0.001 | <0.001 | <0.001 | <0.001 | <0.001 |
| Chy  | 20   | <0.003 | 0.12   | <0.003 | 0.02   | <0.003 | 0.12   | <0.003 | <0.003 | <0.003 | <0.003 | <0.003 | <0.003 |
| BbF  | 0.2  | <0.001 | 0.24   | <0.001 | <0.001 | <0.001 | 0.08   | <0.001 | <0.001 | <0.001 | 0.05   | 0.13   | <0.001 |
| BkF  | 2    | <0.001 | 0.23   | <0.001 | <0.001 | <0.001 | <0.001 | <0.001 | <0.001 | <0.001 | <0.001 | <0.001 | <0.001 |
| BaP  | 0.02 | 0.05   | 1.08   | <0.001 | <0.001 | <0.001 | <0.001 | <0.001 | <0.001 | 0.08   | <0.001 | <0.001 | <0.001 |
| DBhaA  | 0.03 | 0.28   | 0.27   | <0.001 | 0.5    | <0.001 | <0.001 | <0.001 | <0.001 | 0.05   | <0.001 | <0.001 | <0.001 |
| BghiP  | -    | 0.14   | <0.001 | 0.4    | <0.001 | <0.001 | <0.001 | <0.001 | <0.001 | <0.001 | <0.001 | <0.001 | <0.001 |
| lcdP   | 0.3  | 0.04   | <0.001 | 0.1    | <0.001 | <0.001 | <0.001 | <0.001 | <0.001 | <0.001 | <0.001 | 0.04   | <0.001 |
| Σ PAHs   |      | 13.28  | 7.45   | 1.3    | 5.04   | 3.76   | 0.29   | 0.33   | 3.14   | 21.26  | 3.27   | 6.66   | 1.58   |

\*Reference General Levels (RGL) of soils with no industrial or urban use. \*\* Sp8 and Sp10 did not show significant results and they have been omitted. Σ PAHs: summation of total PAHs. Limits of detection according to García-Delgado et al. (2013).

**Table 3** Significant Pearson's correlation coefficient (r) between mineralogical composition and PAHs

| *PAHs | Sm-di(Al) | Sm-tri(Mg) | Sep     | Ill     | Qtz    | Mc      | Ab      | Cal     | Dol    | Σclay min |
|-------|-----------|------------|---------|---------|--------|---------|---------|---------|--------|-----------|
| Naph  | -         | -          | 0.95*** | -       | -      | -       | -       | -       | 0.68** | -         |
| Acy   | 0.75**    | 0.94***    | 0.65*   | 0.80**  | -      | -       | -       | -       | -      | 0.91***   |
| Ace   | 0.82***   | 0.96***    | 0.65*   | 0.71**  | -      | -       | -       | -       | -      | 0.90***   |
| Flu   | 0.74**    | 0.65*      | -       | 0.64*   | -      | -       | -       | -       | -      | 0.69**    |
| Phe   | 0.75**    | 0.85**     | -       | 0.77**  | -      | -       | -       | -       | -      | 0.82***   |
| Ant   | 0.82***   | 0.96***    | -       | 0.91*** | -      | -       | -       | -       | -      | 0.93***   |
| Fla   | -         | -          | -       | -       | 0.75** | 0.87*** | 0.84*** | -0.73** | -      | -         |
| Pyr   | -         | -          | -       | -       | -      | -       | -       | -       | -      | -         |
| BaA   | -         | -          | -       | -       | 0.68*  | -       | -       | -       | -      | -         |
| Chr   | -         | -          | -       | 0.73**  | -      | -       | -       | -       | -      | -         |
| BbF   | -         | 0.78**     | 0.76**  | 0.71**  | -      | -       | -       | -       | -      | 0.76**    |
| BkF   | 0.81***   | 0.96***    | -       | 0.91*** | -      | -       | -       | -0.58*  | -      | 0.93***   |
| BaP   | 0.82***   | 0.96***    | -       | 0.91*** | -      | -       | -       | -0.59*  | -      | 0.94***   |
| DBhaA | -         | -          | -       | -       | -      | -       | 0.62*   | -       | -      | -         |

\* p ≤ 0.05; \* \* p ≤ 0.010. \* \* \* p ≤ 0.001. Only clay minerals that present significant correlation coefficients have been included



**Table 4** Significant Pearson's correlation coefficient (r) between mineralogical composition and trace elements

| Trace elements | Sm-di(Al) | Sm-tri(Mg) | Ill     | Qtz    | Mc     | Ab    | Cal     | Σclay min |
|----------------|-----------|------------|---------|--------|--------|-------|---------|-----------|
| Li             | 0.90***   | 0.87***    | 0.77**  |        | -      | -     |         | 0.87**    |
| Be             | -         | -          |         | -      | -      | -     | -       | -         |
| B              | -         | -          |         | 0.72*  | 0.75** | 0.64* | -0.72*- | -         |
| Sr             | -         | -          | -       |        | -      | -     | -       | -         |
| Y              | 0.69*     | 0.64*      | 0.67*-  | -      | -      | -     | -0.62*  | 0.63*     |
| Ag             | -         | -          |         | 0.72*  | 0.79** | 0.68* | -       | -         |
| Cd             | -         | -          |         | 0.73*  | 0.79** | 0.68* | -       | -         |
| Ba             | -         | -          | 0.68*   | -      | -      | -     |         | 0.62*-    |
| La             | 0.78**    | 0.74**     | 0.75**  | -      | -      | -     | -0.69*  | 0.74**    |
| Ce             | 0.81**    | 0.79**     | 0.76**  | -      | -      | -     | -0.65*  | 0.79**    |
| Tl             | -         | -          |         | 0.73** | 0.80** | 0.71* | -       | -         |
| Bi             | -         | -          |         | 0.71** | 0.81** | 0.67* | -0.61*  | -         |
| Th             | 0.72*     | 0.77**     | 0.76**  | -      |        | -     | -0.76** | 0.74**    |
| U              | 0.75**    | 0.88***    | 0.92*** | -      |        | -     | 0.67*   | 0.84***   |
| Al             | 0.65*     | 0.61**     | -       | -      |        | -     |         | 0.63*     |
| Sc             | 0.72*     | 0.73**     | 0.70*   | -      |        | -     | -0.61*  | 0.72*     |
| V              | -         | 0.68*      | -       | -      |        | -     | -       | 0.68*     |
| Cr             | -         | 0.62*      | -       | -      | -      | -     | -       | -         |

\*  $p \leq 0.05$ ; \* \*  $p \leq 0.010$ . \* \* \*  $p \leq 0.001$ . Only metals and clay minerals that present significant correlation coefficients have been included.

**Table 4.** Concentrations of trace elements (mg/Kg)

| Metal | RGL* | Sp1   | Sp2   | Sp3    | Sp3   | Sp4    | Sp6    | Sp7    | Sp8    | Sp9    | Sp10   | Sp11   | Sp13   | Sp14   |
|-------|------|-------|-------|--------|-------|--------|--------|--------|--------|--------|--------|--------|--------|--------|
| Li    | -    | 24.3  | 178   | 11.1   | 32.9  | 53.8   | 37.3   | 27.8   | 17.6   | 101.5  | 107.8  | 132.4  | 39.9   | 69.2   |
| Be    | 2    | 2.2   | 2     | 0.3    | 0.6   | 0.9    | 1      | 0.7    | 0.4    | 1.2    | 1.3    | 1.7    | 0.5    | 0.6    |
| B     | -    | 15.5  | 5     | 3.2    | 5.8   | 2.2    | 2.4    | 2.5    | 1.8    | 3.8    | 4.3    | 1.4    | 1.4    | <0.01  |
| Sr    | -    | 43.9  | 60.3  | 309    | 544   | 240    | 340.4  | 1271   | 726.9  | 35     | 363.1  | 353    | 141.4  | 276    |
| Y     | -    | 12    | 14.9  | 3.5    | 6.2   | 8.6    | 8.8    | 9      | 6.6    | 10.7   | 10.6   | 12.4   | 4      | 6.7    |
| Ag    | 5    | 1.6   | 0.1   | < 0.01 | 0.5   | < 0.01 | < 0.01 | < 0.01 | < 0.01 | < 0.01 | < 0.01 | < 0.01 | < 0.01 | < 0.01 |
| Cd    | 3    | 1.3   | <0.01 | <0.01  | 0.4   | <0.01  | <0.01  | <0.01  | <0.01  | <0.01  | <0.01  | <0.01  | <0.01  | <0.01  |
| Ba    | 4200 | 138.8 | 51.9  | 93.4   | 167.5 | 86.2   | 109.9  | 141.5  | 76.6   | 133.7  | 195    | 134.8  | 128.2  | 82.3   |
| La    | -    | 14.4  | 20.7  | 5.3    | 6.7   | 11     | 11.3   | 12.3   | 9.1    | 14.2   | 13.9   | 15     | 6.5    | 9.6    |
| Ce    | -    | 29.5  | 44.6  | 13.4   | 14.1  | 22.8   | 22.7   | 24.9   | 20.2   | 29.6   | 30.3   | 35.9   | 15.9   | 23     |
| Tl    | 2    | 1.7   | 0.3   | < 0.01 | 0.4   | <0.01  | 0.1    | 0.1    | 0      | < 0.01 | < 0.01 | 0.1    | < 0.01 | < 0.01 |
| Pb    | 75   | 11.4  | 16.1  | 15.8   | 11.3  | 13.9   | 17.3   | 15.3   | 12.4   | 11.7   | 1.5    | 7.2    | 8.9    | 9.5    |
| Bi    | -    | 2.5   | 0.8   | < 0.01 | 0.6   | <0.01  | 0.3    | 0.1    | 0.1    | 0.2    | 0.2    | 0.5    | < 0.01 | < 0.01 |
| Th    | -    | 8.8   | 12.2  | 2.2    | 2.3   | 3.7    | 4.4    | 4.9    | 4.4    | 6.3    | 6.4    | 7.9    | 2.9    | 3      |
| U     | -    | 3.4   | 10.6  | 0.6    | 2.3   | 1.2    | 3.2    | 1.7    | 1.8    | 1.6    | 1.7    | 2      | 0.8    | 0.9    |
| Al    | -    | 7301  | 17241 | 6689   | 1697  | 8104   | 11990  | 13126  | 12437  | 16652  | 17345  | 16619  | 9157   | 10641  |
| Sc    | -    | 2.1   | 3.6   | 0.6    | 0.5   | 1.1    | 1.4    | 2.3    | 1.8    | 2.3    | 2.3    | 2.7    | 0.8    | 0.8    |
| V     | 37   | 11.1  | 23.9  | 10.2   | 3.2   | 5.6    | 13.3   | 16.4   | 14.6   | 20.3   | 20.2   | 19.4   | 17.6   | 14.5   |
| Cr    | 90   | 8.1   | 12.7  | 5.9    | 3.8   | 4.3    | 8.3    | 10.8   | 9.8    | 10.7   | 10.9   | 12.8   | 6      | 7.3    |

|    |      |       |       |      |       |       |       |       |       |      |      |       |       |       |
|----|------|-------|-------|------|-------|-------|-------|-------|-------|------|------|-------|-------|-------|
| Mn | 690  | 153.4 | 239.7 | 152  | 335.1 | 181.4 | 264.5 | 273.1 | 264.6 | 46.6 | 25   | 272.6 | 111.8 | 174.5 |
| Ni | 405  | 4.8   | 3.4   | 5.8  | 2.2   | 2.7   | 6     | 7.2   | 6.3   | 6.3  | 6.5  | 8.1   | 4.8   | 5     |
| Cu | 80   | 5.6   | 7     | 235  | 4.2   | 3.6   | 10.8  | 11.8  | 8.8   | 7.3  | 7.2  | 11.1  | 9.2   | 81.4  |
| Zn | 1170 | 39.5  | 50    | 43.1 | 13.9  | 17.7  | 53.3  | 44.9  | 42.1  | 41.1 | 46.4 | 54    | 30.2  | 121.5 |
| As | 24   | 53.6  | 57.6  | 52.5 | 3.1   | 49.4  | 55.4  | 61.1  | 54.1  | 58.2 | 55.3 | 63    | 53.4  | 104   |
| Se | 85   | 15.4  | 5.6   | 9.8  | <0.01 | 1.4   | 9.6   | 7.6   | 6     | 9.5  | 17.8 | 12.4  | 8.8   | 13.9  |

---

\*Reference General Levels (RGL) of soils with no industrial or urban use. Sp5 presented concentrations below of LD and it has been omitted